

Analysis of the Modeling Outputs of Shape Factor Effect on Flow Structure between Bridge Piers

Shaker Abdulatif Jalil

Water Resources Engineering Department, College of Engineering, University of Duhok
shaker.abdulatif@uod.ac

Abstract

The submerged flow through piers is a weak turbulent flow. In this flow viscosity damps the flow fluctuations caused by obstacle. The flow conditions are affected substantively by pier shape. For viewing the structural characteristics of flow, twenty two different piers shape has been studied experimentally and modeled numerically. Classical k-ε turbulence model has been employed and comparison has been carried between predicted free surface profiles and laboratory measurements and so has been done with the discharge. The determinants of flow structure that predicted such as viscous length, turbulent energy, turbulence energy percent, turbulent dissipation, energy coefficient and momentum coefficient have been investigated. The investigation leads that these determinants are well reflectors for pier shape and they are highly correlated to flow discharge and Froude number with adjusted coefficient of determination equals to 0.957 and 0.949 respectively. Statistical results show that piers of sudden tail expansion cause an average increase of 16% and 8.5% in the relative values of energy and momentum coefficients respectively compared with gradually expanded, while an average increase of 2%, 23% and 6% in maximum values of viscous length, turbulent dissipation and turbulence energy percent respectively. In addition 10 volumetric shape factors have been calculated and then automatic linear regression has been carried with the structural determinants. The adjusted \bar{R}^2 of five shape factors have exceeded the 80% and the best one is the elongation shape factor.

Keywords: Pier shape, Turbulent dissipation, Turbulent model, Viscous length, VOF model.

الخلاصة

تحليل مخرجات النمذجة لتأثير عامل الشكل على هيكل الجريان بين أعمدة الجسور
الجريان المغمور المتدفق بين اعمدة الجسور هو ضعيف الاضطراب. تعمل قوى اللزوجة على تهدئة وتخفيف حدة الاضطرابات والتذبذب الناتجة من تأثير العقبات. كما تتأثر ظروف الجريان بشكل الاعمدة. ولعرض دراسة الاختلافات في هيكلية الجريان فقد تم اختبار 22 شكلا مختلف من الاعمدة مختبريا ونمذجتها عدديا باستخدام خوارزمية الاضطراب الكلاسيكية (K-ε) لمحاكات التدفق واجريت مقارنة بين مخرجات المحاكات لمناسيب السطح الحر والقياسات المختبرية وكذلك مع قيم التصريف. تم استنباط محددات هيكل الجريان من نتائج المحاكات وكانت الطول اللزج، والطاقة المضطربة، ونسبة الطاقة المضطربة، والتبديد المضطرب، ومعامل الطاقة، ومعامل الزخم. لقد تبين ان هذه الحدودات تعكس بشكل جيد تأثير اشكال الاعمدة وترتبط ارتباطا وثيقا بالتصريف وعدد فرود بمعامل التحديد المصحح يساوي 0.957 و 0.949 على التوالي. وأظهرت النتائج الإحصائية أن الأعمدة ذات التوسع المفاجئ تؤدي إلى زيادة متوسطة نسبتها 16% و 8.5% في القيم المعاملات النسبية للطاقة الزخم على التوالي مقارنة مع التوسع التدريجي في شكل الأعمدة، في حين أن متوسط الزيادة 2% و 23% و 6% في القيم القصوى كل من الطول اللزج، التبديد المضطرب والطاقة المضطربة على التوالي. كما وتم حساب عشرة معاملات شكل حجمية لابعدية وإيجاد الإنحدار الخطي المتعدد مع المحددات اعلاه حيث تجاوزت خمسة معاملات شكل القيمة 80% لمعامل التحديد المصحح (\bar{R}^2 adj). وكان أفضل معاملات الشكل تمثيلا لهيكل الجريان هو معامل الاستطالة.

الكلمات المفتاحية: شكل أعمدة الجسور ، التبديد المضطرب، نموذج المضطرب، الطول اللزج، نموذج VOF.

Introduction

Piers are a fundamental part of bridges and some hydraulic structures. Piers exist nearly everywhere in the world where there is a flow of water. Piers cause a changes in flow due to blocking portion of flow area, the changes appear as backwater upstream, energy loss and in scouring of some bed materials, these changes have been early stated in original literatures as (Chow,1959; Henderson ,1966; French ,1987). Experimental

study by (Kassem; 2006) on backwater rise due to piers and comparison with earlier literatures shows that the main factors affect the backwater rise are type of flow, discharge value, geometry and shape of pier. Modeling of flow structure based on experimental data show that the three dimensional hydrodynamic equation can simulate turbulent flow as laboratory studies (Blumberg *et.al.*,1992). Numerical solution of Reynolds equations with Boussinesq approximation using porosity method for evaluating water surface profile shows a good agreement with the experimental data of Groyne in rectangular channel, the agreement based on the prediction of iso-lines, dynamic pressure and reattachment length (Ouillon and Dartus, 1997). Flow between cylindrical obstacles was simulated using shallow water equations in two-dimensional modeling by (Szydlowski, 2011) which showed a successful method for two types of flow subcritical and supercritical. The measurement of discharge and instantaneous velocity distribution based on an error-minimized application in open channels has been studied by (Bares *et. al.*, 2008) using new technology methods of ultrasonic Doppler. The study shows average relative error is about 3.22% and its value increases as the flow depth increases. (Yokoyama *et.al.*,2004) studied the structure of environmental flow and discharge in a river by integrating the distribution of the velocity which was measured by UVP and compared with the pipe flow. The study shows good agreement with a difference about 10% between them. (Aldebakh and Inaam, 2007) used portable prism to measure the discharge in rectangular channel, the study shows that prediction of the discharge in free flow has higher accuracy than in submerged flow. Drag coefficient on bridge deck by CFD has been studied by (Patil *et.al.*, 2009), the experimental drag has been compared with the calculated values from k- ϵ Renormalization Group turbulent model which shows successful results and an improvement can be held on it by using Large Eddy Simulation (LES) to get the best results. Reynolds stress terms have been modeled by (Baranya *et.al.*, 2012) using k- ϵ model with curvilinear nested grid system to study the structure of flow surrounding circular piers, comparison with laboratory test shows a good agreement with measurement of velocity, profiles, location of flow separation and shear stress. (Pun and Law, 2015) had simulated the effect of bridge piers on the tidal current in channels and concentrated on the flow of contaminants, the study concludes that tidal force simulation shows that the energy losses due to bridge piers reduce the flow especially of the upper surface layers. (Ducrocq *et.al.*, 2015) studied the flow structure in some kind of fish passes and focusing on velocity distribution which affects the migratory of fishes is noticed.

Large numbers of studies were carried out on the shear stress and vortices near obstacles, (Chrisohoides *et.al.*, 2003) studied the vortices caused by bridge abutments on a flat bed experimentally and by simulation using k- ϵ turbulence model. The study based on visualizing comparison of the footprints and scouring process. (Teruzzi *et.al.*, 2006) studied the flow structure around piers and conclude that vortex structure induced by obstacle has the character of high vortex intermittency and the locations of the maximum values for shear stress and vortices near the obstacle edges. (Aghaee and Hakimzadeh, 2010) conclude that large eddy turbulence model (LES) can simulate bed shear stress more intensive when compared with the predicted by k- ϵ model, moreover the LES model shows a better result in predicting horseshoe and Lee wake vortex shedding, the study based on experimental data validation of horizontal flow velocity. The free surface profile changes caused by piers has been simulated by (Kocaman *et.al.*, 2010) successfully by deploying LES and k- ϵ turbulence models, but a refined grid is needed in LES model, these models are powerful of the commercial FLOW-3D software.

The RNG k-ε model also shows a good agreement with experimental data for simulating turbulence properties of flow caused by spur dikes (Acharya *et.al.*, 2013). Numerical studies go deeply into details of flow structure as the generation of vortex near obstacle. The horseshoe vortex three dimensional model for predicting location and shape is forwarded by (Paik *et.al.* ,2007 ; Keshavarzi *et.al.*,2014) carried out a study on scouring and deposition pattern around single circular bridge pier using the transition probabilities, the investigation based on the effect of three turbulent kinetic energy components using an Acoustic Doppler Velocity meter, the study show physical structural for the flow process around piers and make it more understandable.

The current study aim to show the effect of pier shape on structural flow changes within the domain of pier existence by validation of numerical model of 22 different pier shapes and to find the reasonable geometric shape factor that can reflect these changes.

Governing Equations

The natural phenomena's are governed by the laws of conservation, which they control the behavior of fluid in state or in motion, and the properties of fluid flow are functions of space and time (Graebel, 2007). When the inertia forces dominate in fluid flow relative to viscous forces, this situation causes turbulent flow generation with chaotic state and random fluctuation of the velocity components with the time, thus all properties of flow such velocity and pressure are in a random nature. The theory of Reynolds decomposition which based on mean steady value of velocity with its fluctuating component, together with the theory of Kolmogorov of micro-scales helps to understand and simplifies the state of turbulent flow then its conservative equations (see Versteeg and Malalasekera , 2007). Without entering in the structure details of turbulent flow and the correlation functions of time scale and spaces. It can be implanted the time average rules which govern fluctuating properties of flow in the instantaneous equations of continuity. The resulting equations are well known since early 1800s as Navier-Stokes. The incompressible flow equations can be written by replacing flow variables (velocity *u* and pressure *p*) by the sum of mean as in equation (1).

$$\mathbf{u} = \mathbf{U} + \mathbf{u}' , \quad u = U + u' , v = V + v' , w = W + w' , \quad p = P + p' \quad \dots \dots (1)$$

According to (Versteeg and Malalasekera , 2007) the replacement of velocity vectors *u* by the sum of means *U* leads to the continuity equation for the mean flow equation (2) and in the same way to the time -average x-momentum equation (3). The other two directions *y*- and *z*- can be written in a similar manner.

$$\text{div } \mathbf{u} = \text{div } \mathbf{U} = 0 \quad \dots \dots (2)$$

$$\frac{\partial U}{\partial t} + \text{div}(UU) + \text{div}(\overline{u'u'}) = -\frac{1}{\rho} \frac{\partial P}{\partial y} + \nu \text{div}(\text{grad}(U)) \quad \dots \dots (3)$$

The terms $\text{div}(\overline{u'u'})$ are appearing in the equation (3) due to the process of time -averaging. These terms related to the convection of momentum transfer due to eddies. Finally equation (3) can be written in another form by placing these terms ($\text{div}(\overline{u'u'})$) on the right hand side to show that the terms are additional turbulent stress reflecting the process of time averaging on the mean flow components as in equation (4).

$$\frac{\partial U}{\partial t} + \text{div}(UU) = -\frac{1}{\rho} \frac{\partial P}{\partial y} + \nu \text{div}(\text{grad}(U)) + \frac{1}{\rho} \left[\frac{\partial(-\rho \overline{u'^2})}{\partial x} + \frac{\partial(-\rho \overline{u'v'})}{\partial y} + \frac{\partial(-\rho \overline{u'w'})}{\partial z} \right] \dots \dots (4)$$

The last terms in equation (4) are known Reynolds stress and the equation is Reynolds-averaged Navier–Stokes. There are many developed turbulence models for solving of these equations. The numerical solution depends on modeling of the extra six terms that reflecting the time average momentum in the equations. However, the numerical turbulence model depends on the number of extra terms of (Reynolds stress) included in calculation which they will affect the complexity and the economy of the model for flow prediction. The classical turbulence models such as k-ε of two terms transport is widely used because it is able to present the general turbulent main flow by one length scale and one time scale. The transport equations of the turbulence kinetic energy, k, and its rate of dissipation, ε, can be presented as follows:

$$\frac{\partial(\rho k)}{\partial t} + \text{div}(\rho k \mathbf{U}) = \text{div} \left[\frac{\mu_t}{\sigma_k} \text{grad } k \right] + 2\mu_t S_{ij} \cdot S_{ij} - \rho \varepsilon \dots \dots \dots (5a)$$

$$\frac{\partial(\rho \varepsilon)}{\partial t} + \text{div}(\rho \varepsilon \mathbf{U}) = \text{div} \left[\frac{\mu_t}{\sigma_\varepsilon} \text{grad } \varepsilon \right] + C_{1\varepsilon} \frac{\varepsilon}{k} 2\mu_t S_{ij} \cdot S_{ij} - C_{2\varepsilon} \rho \frac{\varepsilon^2}{k} \dots \dots \dots (5b)$$

$$\mu_t = \rho C_\mu \frac{\varepsilon^2}{k} \dots \dots \dots (6)$$

Where:

Sij = the mean of deformation

C_{1ε}, C_{2ε}, C_μ = constants having the values of 1.44, 1.92 and 0.09, respectively

σ_k and σ_ε = Turbulent Prandtl numbers for k and ε having the values of 1.0 and 1.3, respectively.

Modeling is the numerical solution of Reynolds-averaged Navier–Stokes equations. Many software packages are developed for computational fluid dynamics such as commercial software FLOW-3D which developed by Flow-Science Incorporation. This package includes volume of fluid (VOF) which can model two phase fluids such as water and air in grid to evaluate the free surface. This package also includes five turbulence models, as the case under study is a turbulent wake flow generated behind an object, this means that there is a slow fluid motion surrounded by a faster fluid flow. The velocity of faster flow decreases in the direction of flow at a certain distance. This situation of flow behavior has been observed during the experimental study, so the popular RANS (k- ε) model fit the needs of the simulation of submerged flow through piers vent to predict flow profile and discharge economically by the use now a day's personal computer.

Numerical Model and Validation

The model set-up was the same for all pier shapes which include the selection of incompressible flow, free surface or sharp interface, gravitational acceleration in the vertical direction, viscous flow, (k- ε) model and nonslip wall shear boundary. The geometrical pier shapes have been prepared in AutoCAD software as STL files and imported to the main domain of flow. The discretization of computational domain has been set to 0.5 cm mish size of aspect ratio equal to 1. This size of grid gave an error in flow profile and in discharge about 1%. The boundary conditions of the domain were fixed as symmetry at the top and the two sides of the channel while the bottom as a wall. The upstream and downstream conditions have been chosen as pressure to be corresponding to values of water depth upstream and downstream experimental measurements. As the package of FLOW-3D is designed to fit time dependent 3-D free flow that is why the default time step control has been selected unless calculation error is

happened. The pressure velocity coupling solver based on two numerical techniques of semi-implicit formulation of iteration: Successive Over Relaxation (SOR) and Generalized minimum residual (GMRES) (Flow-3D , 2012). As documented in the manual the two solver algorithms show fairly similar results. The SOR algorithm is similar to Jacobi which runs slightly faster than the second algorithm GMRES which solves fully coupled equations system.

The experimental work was carried out in a horizontal rectangular flume with flap tail gate which could control the downstream depth conditions. The working length is 5 m; the width is 0.3m and 0.35m depth. The models of piers were carefully carved from hard teak wood there surface were smoothed and polished. The tested pier where 22 different shapes, all pier models had made of 5 cm width to fit practical contraction ratio of 0.667 and 30 cm height as shown in figure (1). Two piers were fixed in the channel cross section with vent equal 10 cm, thus a constant contraction ratio of $(20/30=0.667)$ was obtained as in figure (2). The surface water profile at the centerline was measured by point gauge carriage for all pier shape models and for about eight discharge runs.

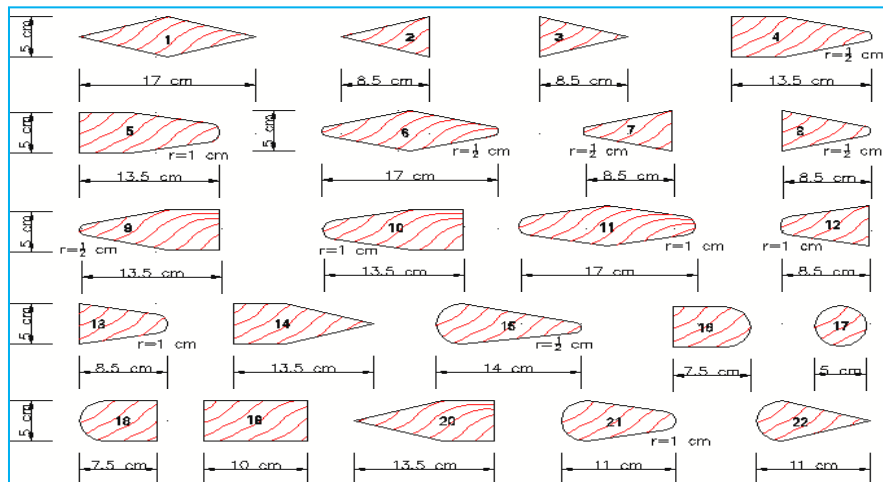


Figure (1) pier shapes and their dimensions of experimental work

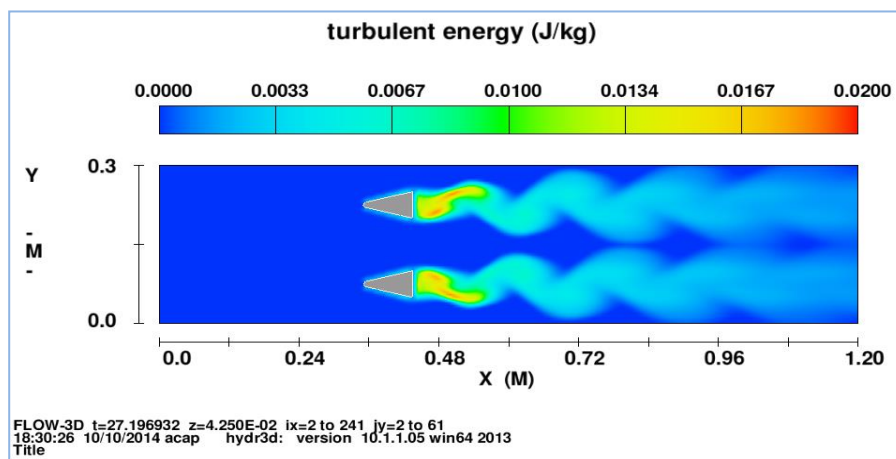


Figure (2) the arrangement of two piers as in experimental laboratory work

Shape Factor

Numerical quantities that represent and describe geometrical shape of objects are known as shape factors. The shape factors are used in many analysis fields such as images, grains and microorganisms; it is also used in engineering such as strength of material and heat transfer. The typical shape factors are Aspect ratio, Circularity, Elongation, Compactness, Waviness, Roundness and Porosity (Yonekawa *et.al.*, 1996). The geometric features of suspended material in river water has been tested by (Billiones *et.al.*, 1999). Billiones study includes amorphous particles that they were recognized after water filtering based on numerous shape factors. Bodies of three-dimensions such as seeds, thickness inters to determine geometric shape factor. (Kaliniewicz *et.al.*, 2012) tested nine different seeds, a model has been proposed of shape factor for each one of these seeds. Three-dimensional shape factors is wildly used in convection heat transfer, general expressions for conduction shape factors were listed in the hand books such as Handbook of Heat Transfer (Rohsenow *et.al.*, 1998). The traditional surface shape factors and proposed ones have been employed in this study. All surface shape factors have been changed into volumetric dimensionless factors by entering the effect of pier length (L_T), perimeter (P) and depth of flow downstream (Y_2). Ten different dimensionless shape factors are proposed with their mathematical formula, they are listed in figure (3).

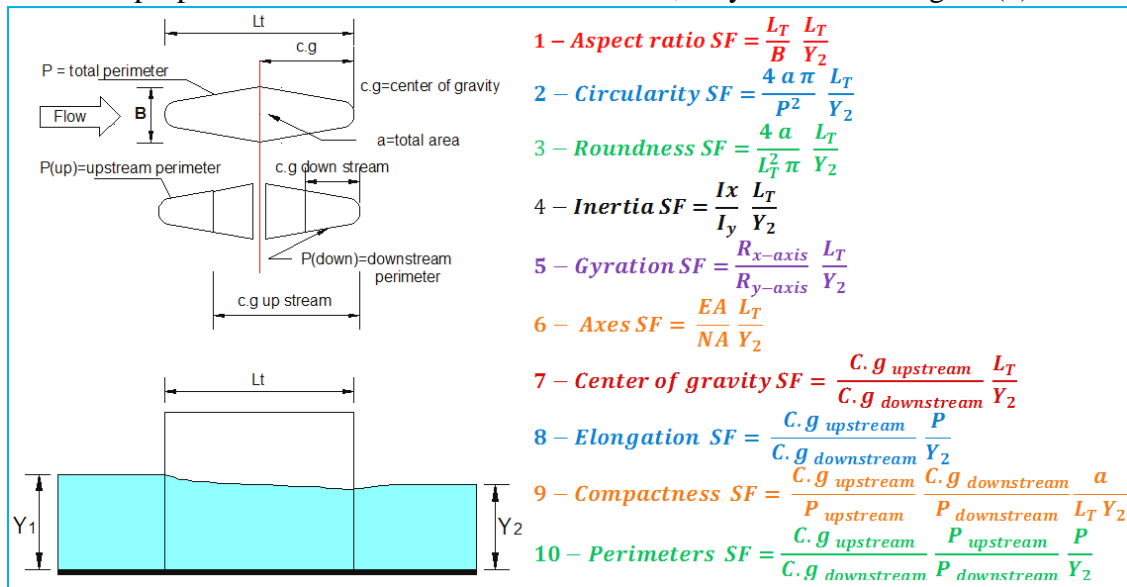


Figure (3) Sketch illustrating pier dimensions and shape factor calculations

Results and Discussion

Twenty two physical pier models have been simulated using the package FLOW-3D®, each pier shape has been run about eight times. Validation was based on experimental measures of discharge and flow depth in the center line between piers. Longitudinal flow profiles are presented in figure (4 and 5) for flow passing through the vent between two different piers; they show both simulation output and the measured flow depth. To check reasonably agreement between the experimental and simulation profile. Statistical comparison has been carried between the measured experimental depths of flow with numerical predicted depth at the same locations.

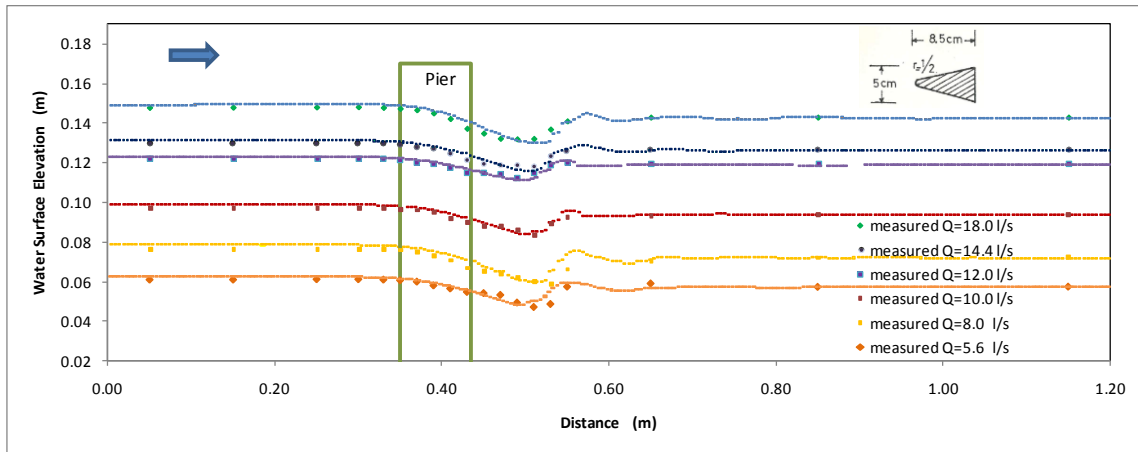


Figure (4) water surface profile, experimental circles numerical dash line

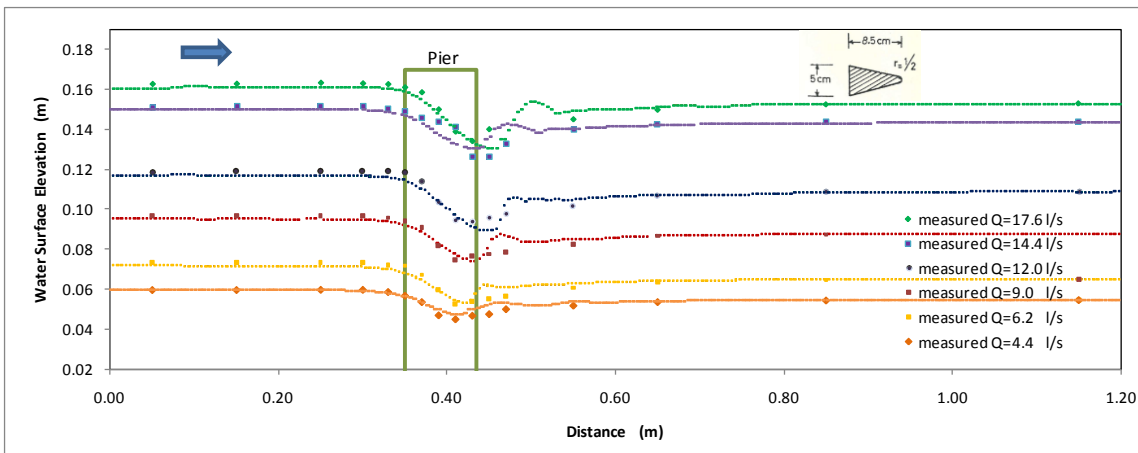


Figure (5) water surface profile, experimental circles numerical dash line

Statistical comparison based on percent of the relative error in the predicted value relative to the measured values of depths is listed in table (1). Table (1) shows the mean percent of the relative error is -0.332% with standard error 0.0449438. The total percent average absolute error is 1.24%. Although the relative percent error is reasonable, but generally this leads to note that the predicted flow depths have a little bit higher values than the measured ones. Piers with sudden expansion at its downstream end such as shape 2, 7 and 12 show higher absolute percent error, while the piers which has streamlined shape without sharp corners such as 15 and 21 show the lowest relative absolute percent error. This little error in predicted depth has been noted at locations directly behind the end of piers. This error is more notable in the case of sudden expansion in pier end and when Froude number increases in subcritical flow.

Table (1) Descriptive Statistics of relative percent error in flow profile

	N	Range	Minimum	Maximum	Mean	Std. Deviation	Variance
	Statistic	Statistic	Statistic	Statistic	Statistic	Std. Error	Statistic
Profile error%	1491	11.8600	-5.9721	5.8879	-.332248	.0449438	1.7354372
Valid N (listwise)	1491						3.012

The relative error in the value of discharge predicted from flux baffles has been calculated. The percent of the relative error in discharge is equal to 0.21% with standard

error 0.18497 as listed in table (2), also the average absolute error is equal to 0.15% which can be considered as reasonable.

Table (2) Descriptive Statistics of relative percent error in predicted discharge

	N	Range	Minimum	Maximum	Mean	Std. Deviation	Variance
	Statistic	Statistic	Statistic	Statistic	Statistic	Std. Error	Statistic
Error %	84	8.8403538	-3.8942782	4.9460756	210896209	.1849474626	1.6950714937
ABS error %	84	4.8388330	.10724265	4.9460756	.974832477	.1526173512	1.3987611281
Valid N (listwise)	84						

The flow structure is a reflection of changes in cross-section area and as that the changes in cross-section depend on pier shape. The changes generate particular flow structure and then modify the water surface profile. Many studies depends on the changes in flow profile to develop empirical equations for estimating flow discharge as (Kassem , 2009). Kassem's investigation concluded that the change in flow profile is mainly affected by contraction ratio and secondary by geometrical shape of two pier ends. In this particular point as each shape cause different change in flow structure, so simulation data outputs may make it possible to explain the changes in the flow structure caused by pier different shapes. For this purpose two surfaces perpendicular to flow direction has been chosen. The first surface is located at the upstream at a distance equal one cell (0.5 cm) from the nose of the pier, while the second surface is located at a distance equal to one cell from the end of the pier. The domain between these two surfaces has the maximum change in velocity vectors. The extreme changes in velocity vectors will have its reflection affect in momentum and energy in each finite volume at that positions. Many simulation outputs emulates structural characteristic properties of flow such as (y^+) which helpful in evaluating the turbulent boundary layer and it is referred to as the viscous length, ($\%trbint$) turbulence intensity percentage which is useful in estimating turbulence level, (tke) turbulent energy and ($dtke$) turbulence dissipation rate which reflects mixing length (see manual) . The visual presentations for three of them in horizontal plane are shown in figure (6).

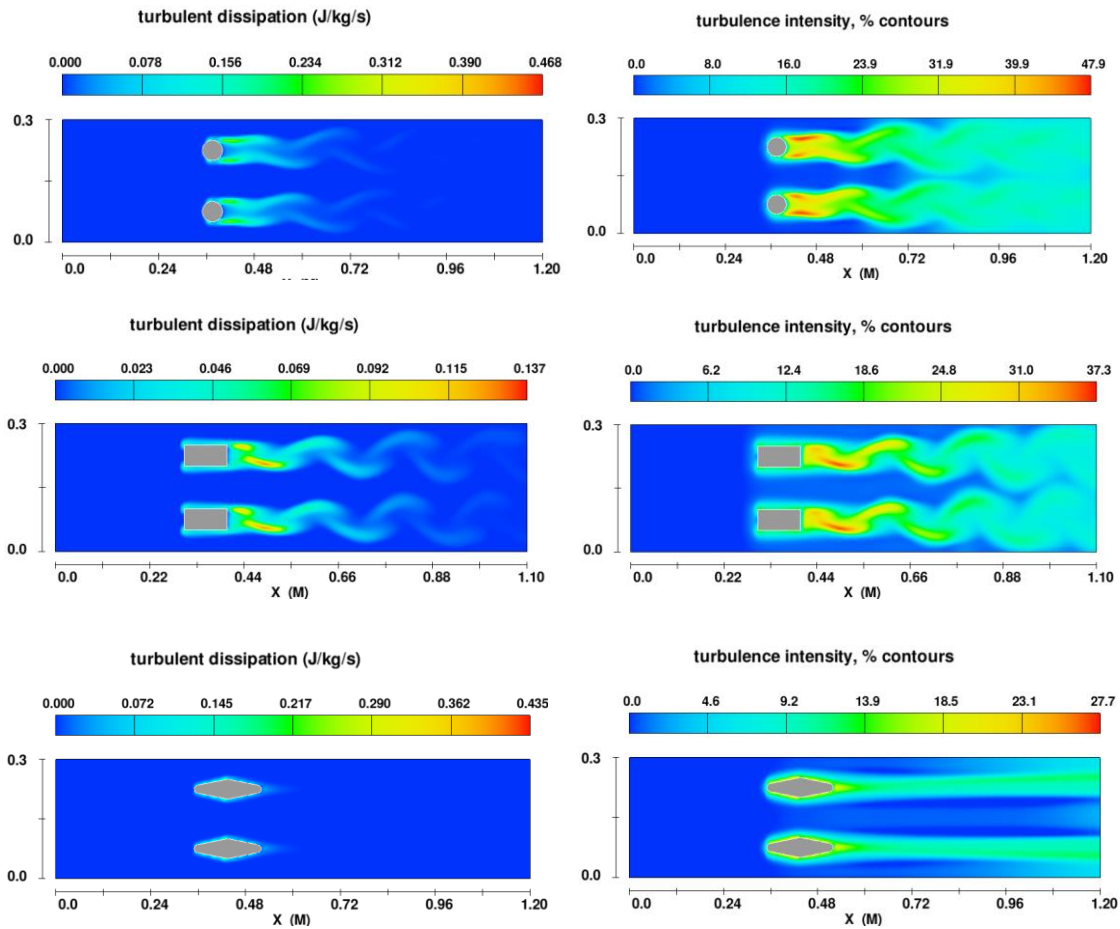


Figure (6) measures for discharge 0.018 m³/s at elevation 0.02 m from channel bed

Three values for each of the mentioned four measures (y^+ , %trbint, tke, dtke) has been found which they are the maximum, the average and the total. This gives 12 independent variables to be included in the analysis. The maximum values of these measures have been found and selected in the domain bounded between pier's nose and tail, while the average and total values of these measures has been calculated at the cross section behind pier's tail. Coefficients of energy and momentum have been calculated at two previously selected cross sections (α_1 , α_2 , β_1 , β_2), also their relative values (α_2/α_1 , β_2/β_1). The total measures characterizing flow structure are 18, and functional relationship can be written as presented in equation (8). To concentrate on the major independent variables those mainly reflect changes in flow structure, so correlation test has been done to the actual discharge (Q_{act}) as dependent variable with 18 measures and also done with Froude number upstream (Fr_1).

$$Q_{act} \text{ or } Fr_1 = f\left(Y^+, Y^+_{average}, Y^+_{total}, tke, tke_{average}, tke_{total}, trbint, trbint_{average}, trbint_{total}, dtke, dtke_{average}, dtke_{total}, \alpha_1, \alpha_2, \beta_1, \beta_2, \alpha_1/\alpha_2, \beta_1/\beta_2\right) \dots \dots \dots (7)$$

The experimental values of discharge were ranging between 4 and 18.4 l/s and the flow conditions were approximately the same for all pier shapes, therefore flow structure differences can be related to effect of pier shapes. The total runs that enter the statistical

analysis were 152 data, which include all 22 pier shapes with their related experimental discharge. The correlation between actual discharge (Q_{act}) and the major independent 18th variables has been achieved by employing the correlation scheme available in SPSS 20 (statistical software package). The highest positive significant correlation coefficient at the 0.01 level (2-tailed) have Y^+ , $dtke_{total}$, Y^+_{total} and tke_{total} while the independent variables $Y^+_{average}$, α_1 , α_2 , β_2 and α_2/α_1 have a negative significant correlation coefficient at the same level. The automatic linear regression improves modeling and accelerates data selection through automatic process to fit predictors; the scheme process is carried as Machine Learning to get the best model fitting (Yang, 2013). The automatic linear modeling for the functional relation in equation (7) leads to the following model presented in equation (8), for which the adjusted coefficient of determination \bar{R}^2 is equal to 0.958.

$$Q_{act} = 13.103 + 0.001Y^+_{total} - 0.559Y^+_{average} + 0.114Y^+ + 0.199dtke_{total} - 219.321dtke_{average} - 19.181\alpha_1 - 14.42\frac{\alpha_2}{\alpha_1} + 13.248\beta_2 + 0.0004trbin_{total} + 7.625\alpha_2 \dots \dots \dots (8)$$

The automatic linear regression gives nearly the same formula as equation (8) for predicting Fr_1 but with different coefficients and also with acceptable adjusted $\bar{R}^2 = 0.949$. It should be noted that not all the predictors in equation (8) has the same importance. The most important predictors are Y^+ , Y^+_{total} , $Y^+_{average}$ and with less importance are α_1 , α_2 which means that the turbulent flow structure is mainly characterized by turbulent boundary layer and coefficient of energy in cross section. Therefore an automatic linear regression has been carried on to generate new models for actual discharge (Q_{act}) and Froude number (Fr_1) with the five important predictors. The linear models show an acceptable adjusted \bar{R}^2 with more than 0.9 as written in equations (10a and 10b).

$$Q_{act} = 1.252 + 0.001Y^+_{total} - 0.893Y^+_{average} + 0.153Y^+ - 3.141\alpha_1 \dots \dots \dots (9 a) \quad Adj. \bar{R}^2 = 0.917$$

$$Fr_1 = 0.150 - 6.425 \times 10^{-6}Y^+_{total} - 0.010Y^+_{average} + 0.002Y^+ - 0.030\alpha_2 \dots \dots (9 b) \quad Adj. \bar{R}^2 = 0.902$$

The interpretation of the above equations (8, 9a, 9b) is that all differences and changes that happens in structural flow are affected by flow rate and pier shape. The structural changes of flow are existed in the velocity distribution, generation of turbulent boundary layer, eddy generation and energy dissipation. All these changes can be visualized to eye from the outputs of numerical simulation. To show how the pier shape affect the structural measures; figure (7) shows the maximum viscous length (Y^+) in the domain between piers and also shows it's increase with the increases of flow rate. The value of (Y^+) is greater than 30 which indicates that inner layer transitions smoothly into the log-law region and it is also largely less than the value(500)that depends on the Reynolds number and thickness of the boundary layer (Flow-3D, 2012).

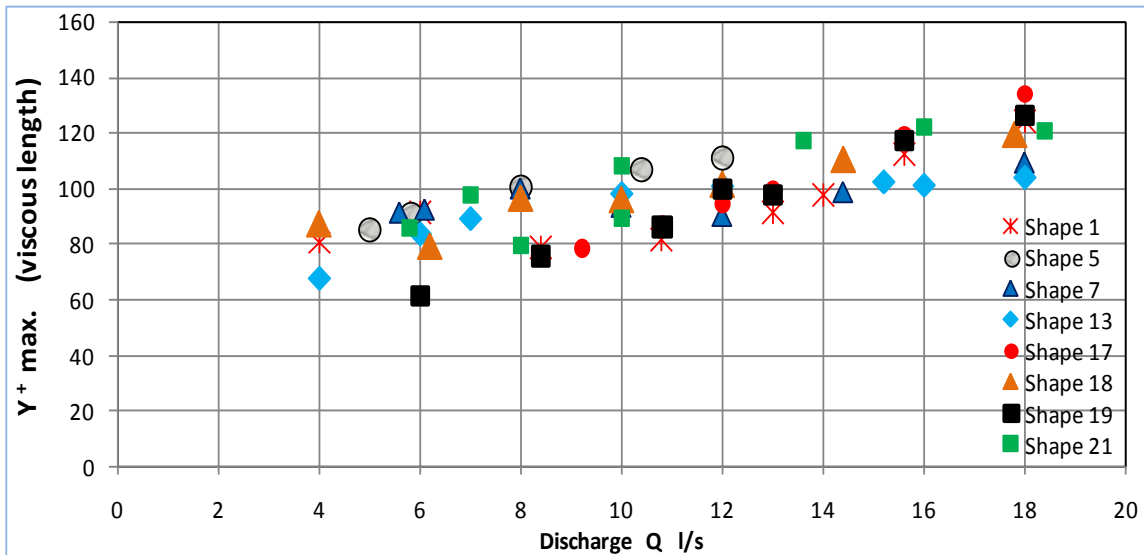


Figure (7) maximum viscous length of the domain between piers

Figure (8) shows the total viscous length in cross section directly after pier tail, also shows the increase in the total viscous length as the flow rate increases. Moreover can be noted that piers which has a sudden expansion tail causes larger total viscous length and its rate of increase is also higher when rate flow increases. The variation of maximum turbulence dissipation rate (dtke) with flow rate is presented in figure (9) which shows that dissipation depend on pier shape and increase with the increases of flow rate.

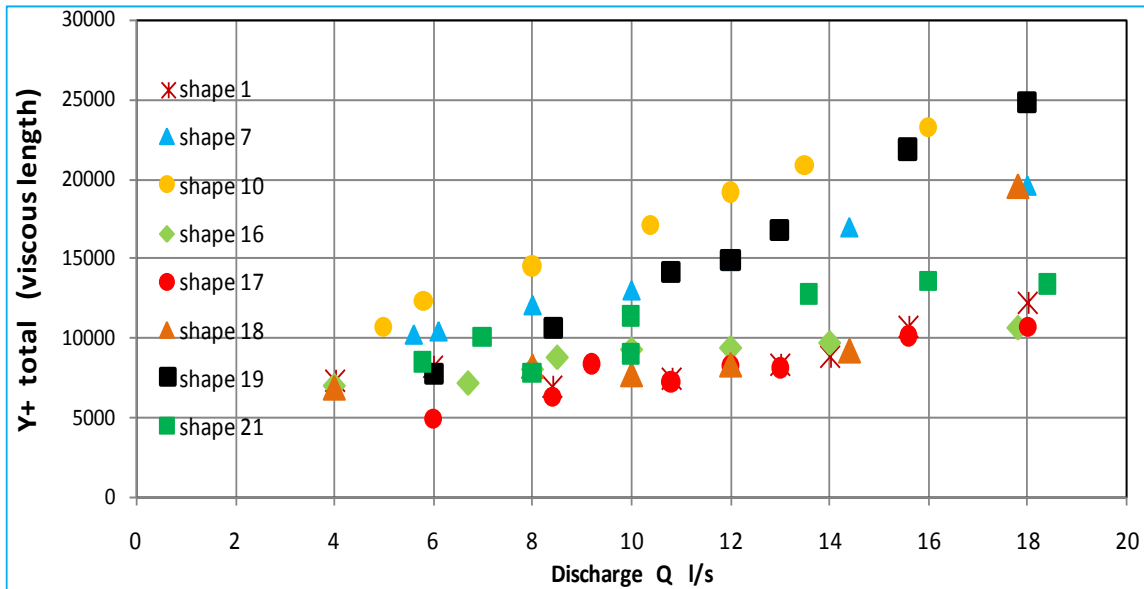


Figure (8) total viscous length at downstream plane

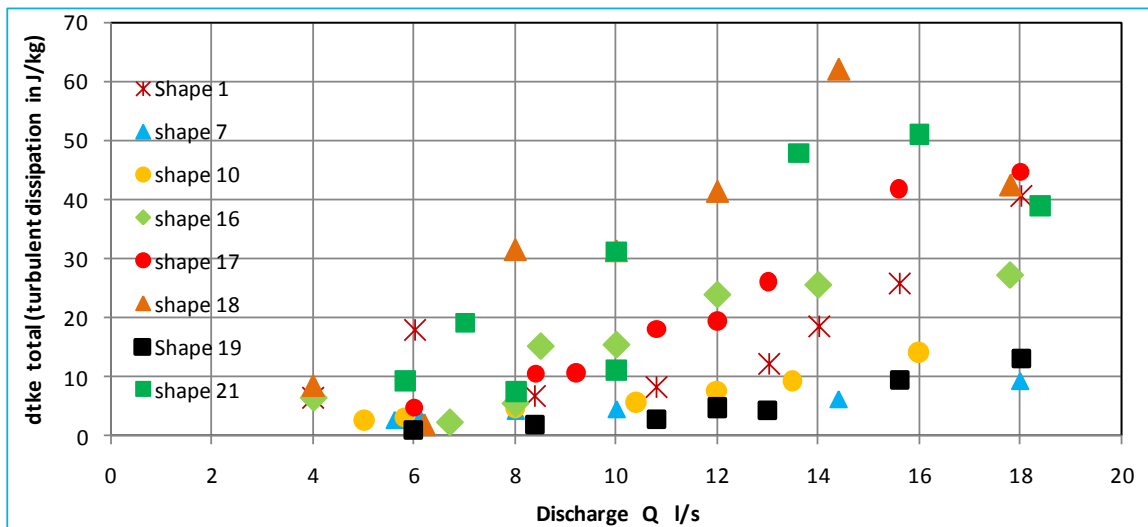


Figure (9) total turbulent dissipation rate at downstream plane

Ten different shape factors have been calculated and listed in figure (3). To study which of these volumetric dimensionless factors can reflect the changes in flow structure; for this purpose automatic linear regression has been applied between each shape factor and the same above structural measures. The adjusted coefficient of determination from the results of automatic linear regression ($\text{adj. } \bar{R}^2$) is listed in table (3) which shows that five shape factors have exceeded the 80% and the best value is for the volumetric elongation shape factor.

Table (3) adjusted coefficient of determination of pier shape factor

Shape Factor	Adjusted \bar{R}^2	Shape Factor	Adjusted \bar{R}^2
1- Aspect ratio SF	0.630	6- Axes SF	0.736
2- Circularity SF	0.824	7- Center of gravity SF	0.828
3- Roundness SF	0.824	8- Elongation SF	0.854
4- Inertia SF	0.550	9- Compactness SF	0.785
5- Gyration SF	0.639	10- Perimeters SF	0.845

The effect of pier shape on some structural properties of flow in the domain bounded between the pier nose and tail can be grouped into two types. The first group which has a sudden expansion tail and the second group has gradually expanded. The statistical results of the averages show that percentage of energy coefficients (α_2/α_1) for the sudden tail expansion piers has higher values of 16% compared with gradually expanded and for β_2/β_1 is 8.5%. The maximum average value of viscous length (Y^+) in the domain increases about 2% and the maximum turbulent dissipation (dtke) increase by 23% while the maximum value of turbulent energy (% trbint) increases by 6% .

Conclusion

Flow through piers vent is affected by pier shape which causes a certain pattern change in flow structure. Experimental and numerical output data lead to the following conclusions and findings:

- Viscous length, turbulent dissipation, energy and momentum coefficients are the major flow structural properties affected by pier shape for a particular discharge.

- The best volumetric shape factor which can reflect structural flow characteristics is the elongation shape factor.
- A pier which has a sudden expansion tail causes an increase in turbulent dissipation (ϵ) by 23%
- A pier which has a sudden expansion tail causes an increase in turbulence energy (k) by 6%.
- Energy and momentum coefficient percentage (α_2/α_1 , and β_2/β_1) increase by 16% and 8.5% respectively for the piers of sudden expansion tail compared with gradually expanded.

References

- Acharya A., Acharya A. and Duan J.G., 2013. Three Dimensional Simulation of Flow Field around Series of Spur Dikes. *International Refereed Journal of Engineering and Science*, 2(7), pp.36–57.
- Aghaee Y. and Hakimzadeh H., 2010. Three Dimensional Numerical Modeling of Flow around Bridge Piers Using LES and RANS. In *Proceedings of the International Conference on Fluvial Hydraulics, Braunschweig, Germany, September 08-10, 2010: River flow 2010*. pp. 211–218.
- Aldebakh A. and Inaam J., 2007. Discharge Measurement in Rectangular Channels Using Portable Prisms. *Engineering and Technology Journal, University of Mosul*, 25(3), pp.132–142.
- Baranya S. , Olsen N R B, Stoesser, T. and Sturm,T., 2012. Three-Dimensional Rans Modeling of Flow Around Circular Piers using Nested Grids. *Engineering Applications of Computational Fluid Mechanics*, 6(4), pp.648–662.
- Bares V., Krajdl J. and Pollert J., 2008. Open-channel Discharge Measurement based on Ultrasonic Doppler Velocity Profiling – Laboratory Experiments. In *6th International Symposium on Ultrasonic Doppler Methods for Fluid Mechanics and Fluid Engineering, Sep 09, 2008 09:00 Prague, Czech Republic*. pp. 25–28.
- Billiones R.G., Tackx M.L. and Daro M.H., 1999. The Geometric Features , Shape Factors and Fractal Dimensions of Suspended Particulate Matter in the Scheldt Estuary (Belgium). *Estuarie, Coastal and Sheif Science*, 48(3), pp.293–305.
- Blumberg A.F., Galperin B. and O'Connor D.J., 1992. Modelling Vertical Structure of Open-channel Flows. *Journal of Hydraulic Engineering - ASCE*, 118(8), pp.1119–1134.
- Chow V. Te, 1959. *Open-channel hydraulics*, Tokyo: International Student Edition, Kogakusha Company, LTD.
- Chrisohoides A., Sotiropoulos F. and Sturm T.W., 2003. Coherent Structures in Flat-Bed Abutment Flow: Computational Fluid Dynamics Simulations and Experiments. *Journal of Hydraulic Engineering - ASCE*, 129(3), pp.177–186.
- Ducrocq T., Chorda J., Cassan L. and Roux H., 2015. Flow around a Single Emerged Cylinder. In *E-proceedings of the 36th IAHR World Congress 28 June – 3 July, 2015, The Hague, the Netherlands*. pp. 1–8.
- Flow-3D, 2012. *Flow-3D Documentation, Release 10.1.0* I. Flow Science, ed.,
- French R.H., 1987. *Open-Channel Hydraulic* 2nd ed., Singapore: McGraw-Hill Book Company.
- Graebel W.P., 2007. *Advanced Fluid Mechanics*, Burlington, MA 01803, USA: Elsevier Ltd.

- Henderson F.M.,1966. *Open Channel Flow*, New York: Macmillan Publishing co.,Inc.
- Kaliniewicz Z. *et.al.*,2012. Determination of Shape Factors and Volume Coefficients of Seeds from Selected Coniferous Trees. *TECHNICAL SCIENCES*, 15(2),pp.217–228.
- Kassem S.E., 2006. Experimental Study of Backwater Rise Due to Bridge Piers as Flow Obstructions. In *Tenth International Water Technology Conference, IWTC10 2006*. Alexandria, Egypt, pp. 319–336.
- Kassem S.E., 2009. Backwater Rise Due to Flow Constriction by Bridge Piers. In *Thirteenth International Water Technology Conference, IWTC 13 2009, Hurghada, Egypt*. pp. 1295–1319.
- Keshavarzi A., Melville B. and Ball J., 2014. Three-dimensional analysis of coherent turbulent flow structure around a single circular bridge pier. *Environ Fluid Mech*, 14, pp.821–847.
- Kocaman S., Seckin G. and Erduran K.S., 2010. 3D model for prediction of flow profiles around bridges. *Journal of Hydraulic Research*, 48(4), pp.521–525.
- Ouillon S. and Dartus D., 1997. Three-Dimensional Computation of Flow around Groyne. *Journal of Hydraulic Engineering - ASCE*, 123(11), pp.962–970.
- Paik J., Escauriaza C. and Sotiropoulos F., 2007. On the bimodal dynamics of the turbulent horseshoe vortex system in a wing-body junction. *PHYSICS OF FLUIDS*, 19(45107), pp.1–20.
- Patil S., Kostic M. and Majumdar P., 2009. Computational Fluid Dynamics Simulation of Open-Channel Flows Over Bridge-Decks Under Various Flooding Conditions. In *Proceedings of the 6th WSEAS International Conference on FLUID MECHANICS (FLUIDS'09), Ningbo, China January 10-12, 2009*. pp. 114–120.
- Pun K.L. and Law S., 2015. Effects of Bridge Pier Friction on Flow Reduction in a Navigation Channel. *Journal of Water Resource and Hydraulic Engineering*, 4(4), pp.326–331.
- Rohsenow W.M., Hartnett J.R. and Young C.I., 1998. *Handbook of Heat Transfer* Third Edit., New York: McG.
- Szydlowski M., Tylek P., and Markowski P., 2011. Numerical Simulation of Open Channel Flow between Bridge Piers. *TASK Quarterly: scientific bulletin of Academic Computer Centre in Gdansk*, 15(3–4), pp.271–282.
- Teruzzi, A., Ballio, F., Salon, S. and Armenio, V., 2006. Numerical investigation of the turbulent flow around a bridge abutment. In *River Flow 2006, Two Volume Set: Proceedings of the International Conference on Fluvial Hydraulics, Lisbon, Portugal, 6-8 September 2006*. pp. 667–672.
- Versteeg H.K. and Malalasekera W., 2007. *An Introduction to Computational Fluid Dynamics* Second Edi., Edinburgh Gate: Pearson Education Limited England.
- Yang H., 2013. The Case for Being Automatic: Introducing the Automatic Linear Modeling (LINEAR) Procedure in SPSS Statistics. *Multiple Linear Regression Viewpoints*, 39(2), pp.27–37.
- Yokoyama K., Kashiwaguma N., Okubo T. and Takeda Y., 2004. Flow Measurement in an Open Channel by UVP. In *4th International Symposium on Ultrasonic Doppler Method for Fluid Mechanics and Fluid Engineering, Sapporo, 6.-8. September, 2004*. pp. 55–58.
- Yonekawa S., Sakai N. and Kitani O., 1996. Identification of Idealized Leaf Types Using Simple Dimensionless Shape Factors by Image Analysis. *Information and Electrical Technologies Div. ASAE*, 39(4), pp.1525–1533.